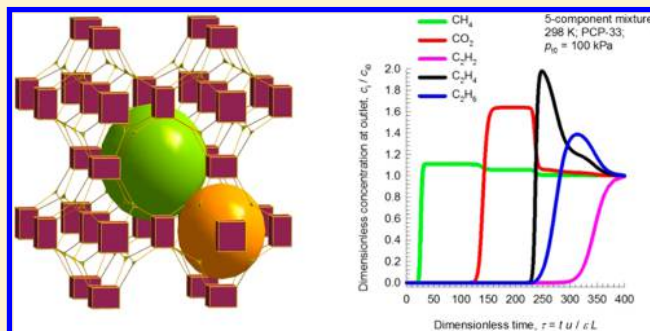


Natural Gas Purification Using a Porous Coordination Polymer with Water and Chemical Stability

Jingui Duan,^{*,†} Wanqin Jin,[†] and Rajamani Krishna[‡][†]State Key Laboratory of Materials-Oriented Chemical Engineering, College of Chemistry and Chemical engineering, Nanjing Tech University, Nanjing 210009, China[‡]Van 't Hoff Institute for Molecular Sciences, University of Amsterdam, Science Park 904, 1098 XH Amsterdam, The Netherlands

S Supporting Information

ABSTRACT: Porous coordination polymers (PCPs), constructed by bridging the metals or clusters and organic linkers, can provide a functional pore environment for gas storage and separation. But the rational design for identifying PCPs with high efficiency and low energy cost remains a challenge. Here, we demonstrate a new PCP, $[(\text{Cu}_4\text{Cl})(\text{BTBA})_8 \cdot (\text{CH}_3)_2\text{NH}_2 \cdot (\text{H}_2\text{O})_{12}] \cdot x\text{Guest}$ (PCP-33 \cdot guest), which shows high potential for purification of natural gas, separation of $\text{C}_2\text{H}_2/\text{CO}_2$ mixtures, and selective removal of C_2H_2 from $\text{C}_2\text{H}_2/\text{C}_2\text{H}_4$ mixtures at ambient temperature. The lower binding energy of the framework toward these light hydrocarbons indicates the reduced net costs for material regeneration, and meanwhile, the good water and chemical stability of it, in particular at pH = 2 and 60 °C, shows high potential usage under some harsh conditions. In addition, the adsorption process and effective site for separation was unravelled by *in situ* infrared spectroscopy studies.



■ INTRODUCTION

Due to the energy crisis and environmental concerns, the efficient storage and separation of C1 and C2 hydrocarbons (CH_4 , C_2H_2 , C_2H_4 , and C_2H_6) have attracted a great deal of research interest. This is because CH_4 with high heat of combustion (55.7 kJ/g) is poised to become one of the most important energy sources in the future.¹ Acetylene and ethylene are widely used as feedstocks in industrial reactions of polymerization, oxidation, alkylation, hydration, oligomerization, and hydroformylation.^{2,3} To produce ethylene, acetylene as the byproduct from the steam cracking of ethane shows deleterious effect to the polyethylene reaction, and also it is well-known to be a highly reactive molecule: it cannot be compressed above 0.2 MPa or it explodes without oxygen, even at room temperature. Furthermore, the separation of $\text{C}_2\text{H}_2/\text{CO}_2$ mixtures is important in industry for production of pure C_2H_2 , which is required for a variety of applications in the petrochemical and electronic industries. The $\text{C}_2\text{H}_2/\text{CO}_2$ separation is particularly challenging in view of the similarity of the molecular dimensions and boiling points.⁴ Thus, the challenges we now face are becoming more practical in nature, that is, how to design and synthesize the safe and effective materials for economic separation.^{5–7}

In order to fully utilize these light hydrocarbons, the separations are generally done by cryogenic distillation, which entails high danger and large energy costs. Recently, in contrast with carbon tube⁸ and zeolites,⁹ a new class of porous materials, porous coordination polymers (PCPs) also called metal–

organic frameworks (MOFs),^{4,10–21} demonstrate significant promise for such task, since their easy tailorability could lead to higher surface and functional pore environments for different recognition abilities of each component.^{22–26} Thus, with great versatility of their structures and pore surface nature, PCP materials have been considered as the most promising candidates for such separations.

Generally, the optimal candidate of PCP materials for gas separation should satisfy at least four important factors:^{27–30} (1) high separation selectivity; (2) high separation capacity; (3) good water and chemical stability; (4) low binding energy. Although recent studies showed that some of the strategies, such as immobilizing the strong recognition sites for higher gas selectivity,^{31–33} improving the pore volume for higher gas capacity,³⁴ and enhancing the coordination strength for stable framework,^{28,35–37} worked very well in each aspect, the disadvantages of these strategies are also very obvious. For example, the net energy cost for the regeneration process will be increased in frameworks with high binding energies (50–90 kJ/mol), but much lower binding energy will result in lower selectivity.³³ In many cases, the modified frameworks are very sensitive to water and offer significantly reduced pore volume. There is a need to optimize the required characteristics and integrate all of these into one PCP framework. Our objective is the construction of porous coordination polymers for a variety

Received: December 16, 2014



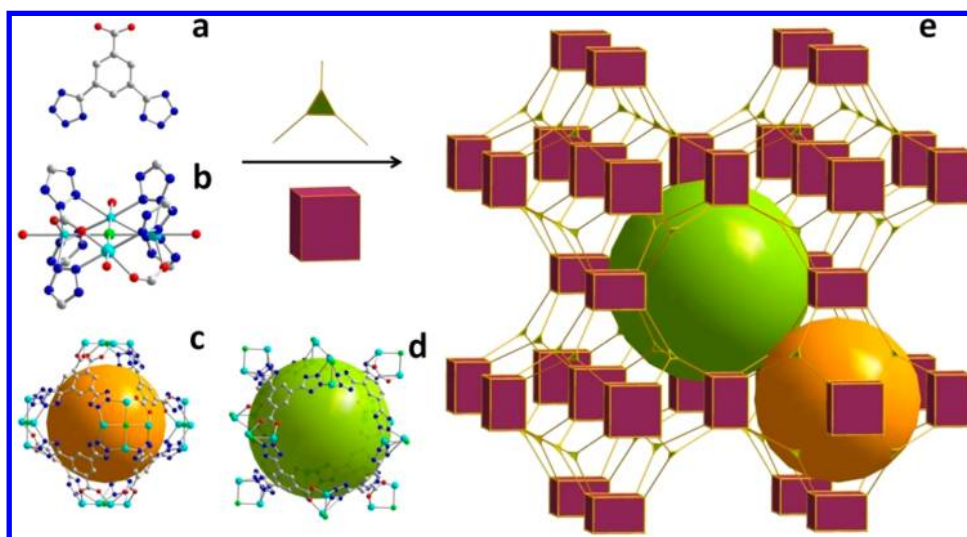


Figure 1. Structure of PCP-33: (a) molecular structure of well designed C_{2v} symmetric ligand (H_3BTBA); (b) the square-planar Cu_4Cl cluster surrounded by six tetrazolate and two carboxylate groups; (c, d) the view of two kinds of cages in PCP-33; (e) the packing view of the 3,8-connected three-dimensional framework derived from the structure of PCP-33.

of applications.^{27–29,38} Recently, we reported two water and chemical stable frameworks for selective capture of CO_2 . The high coordination number of the La^{3+} atom and well-packed organic walls provide the increased bond energy and hydrophobic environment for a water-resistant framework. However, the heats of adsorption are too low to achieve higher performance for gas separation. In order to further optimize the function of the candidate material, herein, we demonstrate a PCP based on a new C_{2v} symmetric ligand (3,5-bis(2*H*-tetrazol-5-yl)-benzoic acid, H_3BTBA) with heterocoordination groups (Figure 1a). The generated PCP, with suitable pore size distributions and exposed open metal sites, exhibits promising characteristics of high separation capacity and high selectivity of light hydrocarbons at room temperature. In addition, the lower binding energy of the framework toward these light hydrocarbons indicates the reduced net costs for material regeneration, and meanwhile, the good water and chemical stability of it shows high potential for usage under some harsh conditions. Furthermore, the adsorption process and adsorption site for separation was well revealed by using an *in situ* infrared spectroscopy study. Thus, PCP-33 is one of the promising candidates that possess good performance characteristics natural gas purification.

EXPERIMENTAL SECTION

General procedures for the experiments, ligand synthesis, and simulations can be found in the Supporting Information.

Synthesis and Structure of PCP-33. For synthesis of $[(Cu_4Cl)(BTBA)_8 \cdot (CH_3)_2NH_2] \cdot (H_2O)_{12} \cdot xGuest$ (PCP-33·*x*Guest), copper(II) chloride (10 mg), H_3BTBA (6 mg), and HCl (30 μ L) were mixed with 2 mL of DMF/ H_2O (5:1) in a 4 mL glass container, and the container was tightly capped with a Teflon vial, and the mixture was heated at 65 °C for 2 days. After cooling to room temperature, the resulting green polyhedral crystals were harvested with high yield (65% based on ligand) and washed by DMF.

Solvothermal reaction of $CuCl_2 \cdot 2H_2O$ with H_3BTBA in DMF/ H_2O containing HCl afforded blue crystals of PCP-33·*x*Guest. Single crystal X-ray diffraction shows that the chloride-centered square-planar $[Cu_4Cl]$ units are linked by eight ligands to form a three-dimensional framework as shown in Figure 1. The cubic sodalite-type framework of PCP-33 is similar as that of Mn-BTT, even though their ligands have different symmetry.³⁹ The size of the open pore is around 11 Å, while

the size of the cross point of the 3-D channel reached 20 Å. In addition, the anionic charge of the framework was balanced by $((CH_3)_2NH_2)^+$, derived from the hydrolysis of DMF in the presence of HCl, which shows a little difference from the counterions $[Mn(CH_3OH)_6]^{2+}$ in Mn-BTT. The total accessible volume of the fully desolvated PCP-33 is ca. 47.4%, calculated using the PLATON program.⁴⁰ The powder X-ray diffraction (PXRD) of the as-synthesized and degassed form of PCP-33 was collected (Figure S6, Supporting Information). With very good reliability factors ($R_p = 0.03306$ and $R_{wp} = 0.04469$), Le Bail analysis of as-synthesized form shows that the refined parameters ($a = 17.5229$ Å) are very close to the data from the single crystal ($a = 17.5355(12)$ Å), reflecting good phase purity and also well-defined structure (Figure S7, Supporting Information). In addition, the peak positions of the degassed form are consistent with its as-synthesized form. Therefore, the framework of PCP-33 is stable even after removing the guest molecules. Thermogravimetric analysis (TG) of PCP-33 shows that PCP-33 is thermally stable up to 200 °C under N_2 atmosphere.

Gas Adsorption. The permanent porosity of desolvated PCP-33 was established by N_2 sorption experiments at 77 K, which exhibits a complete reversible type-I isotherm (Figure 2). The estimated apparent Brunauer–Emmett–Teller surface area is ~ 1248 $m^2 \cdot g^{-1}$ (Langmuir surface ~ 1419.3 $m^2 \cdot g^{-1}$). The calculated pore size distributions according to N_2 isotherm (NLDFT/GCMC method) are in the range 9–22 Å, which matches well the parameters of the

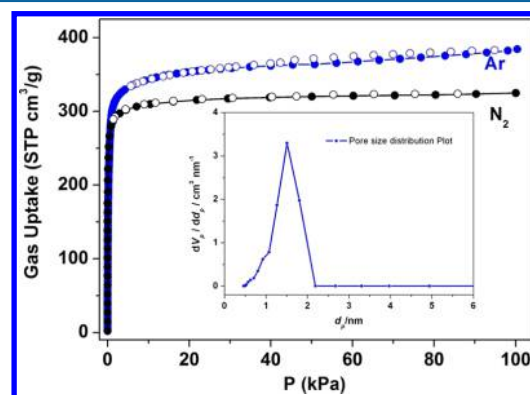


Figure 2. N_2 and Ar adsorption isotherms of PCP-33 at 77 and 87 K. Inset, calculated pore size distributions. The calculated pore volume reached 0.50 $cm^3 \cdot g^{-1}$.

crystal structure. The total pore volume calculated from the maximum amount of N_2 adsorbed is $0.50 \text{ cm}^3 \cdot \text{g}^{-1}$. The C_1 and C_2 hydrocarbons and CO_2 adsorption isotherms of PCP-33 at 273 and 298 K have been collected and fitted (Figure 3). The Langmuir–Freundlich parameters

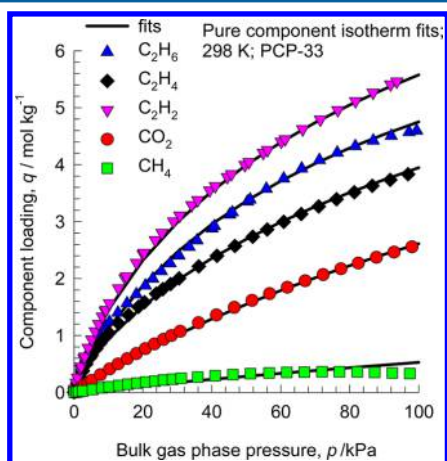


Figure 3. Comparison of absolute component loadings for CH_4 , C_2 hydrocarbons, and CO_2 at 298 K in PCP-33 with the isotherm fits.

for each pure component isotherms in PCP-33 are provided in Table S1, Supporting Information. The adsorption hierarchies of these five gases are very distinct, indicating good separability. The total uptake of C_2H_2 , C_2H_4 , C_2H_6 , CO_2 , and CH_4 in PCP-33 reached 121.8, 102.4, 86.8, 58.6, and $6.9 \text{ cm}^3 \cdot \text{g}^{-1}$, respectively, at 1 bar and 298 K. In addition, all of the isotherms are completely reversible, and no hysteresis is observed. Thus, these results motivated us to examine the potential application of PCP-33 for C_1 and C_2 hydrocarbon and CO_2 separation, given the fact that these five molecules have comparable molecular sizes (Table S2, Supporting Information).

Adsorption Selectivity. The ideal adsorbed solution theory (IAST) of Myers and Prausnitz⁴¹ was employed to predict multicomponent adsorption behaviors from the experimental pure-gas isotherms. Figure 4 presents IAST calculations of the component

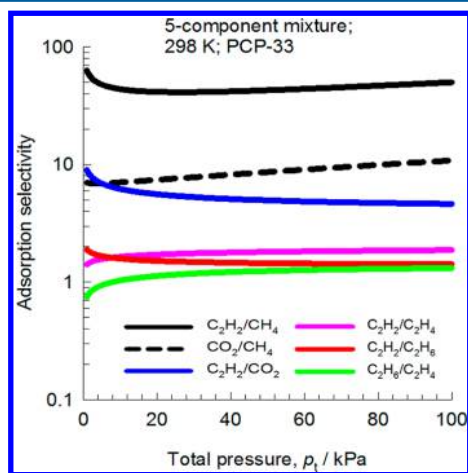


Figure 4. IAST calculations of CH_4 , C_2H_2 , C_2H_4 , C_2H_6 , and CO_2 adsorption selectivities in PCP-33 at 298 K.

loadings for CH_4 , C_2H_2 , C_2H_4 , C_2H_6 , and CO_2 for adsorption of a five-component equimolar mixture in PCP-33 at 298 K. The IAST calculations show the following loading hierarchies at 100 kPa. On the basis of the component loadings, we calculate the selectivities of separation of the six constituent binary pairs: C_2H_2/CH_4 , C_2H_2/C_2H_4 , C_2H_2/C_2H_6 , C_2H_2/CO_2 , C_2H_4/C_2H_6 , and CO_2/CH_4 . The C_2H_2/CH_4 selectivity is the highest and falls in the range of 40–65, indicating the

potential for separation. The predicted CO_2/CH_4 selectivity, as well as the C_2H_2/CO_2 selectivity, is around 6–10. In addition, we note that the equimolar C_2H_2/C_2H_4 , C_2H_2/C_2H_6 , and C_2H_6/C_2H_4 selectivities are all close to unity, showing the separation of individual components of C_2 hydrocarbons is difficult. Thus, the IAST calculations in Figure 4 demonstrate high potential for natural gas purification, as well as the possibility for selective removal of CO_2 from C_2 hydrocarbons and separation of C_2H_2/CO_2 mixtures at room temperature.

Isosteric Heat of Adsorption. To understand such high separation ability better, the adsorption enthalpies were calculated. The binding energies of C_2H_2 , C_2H_4 , C_2H_6 , and CO_2 in PCP-33 are reflected in the isosteric heat of adsorption, Q_{st} . These values were determined using the pure component isotherm fits. Figure 5 presents

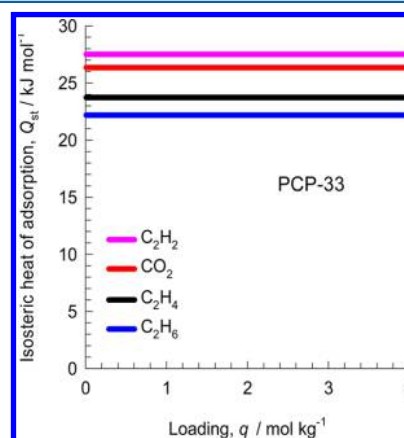


Figure 5. Isosteric heats of adsorption for C_2H_2 , C_2H_4 , C_2H_6 , and CO_2 in PCP-33. The determination of the Q_{st} is based on the Clausius–Clapeyron equation.

data on the loading dependence of Q_{st} for C_2H_2 , C_2H_4 , C_2H_6 , and CO_2 in PCP-33. We note that the binding energies are in the narrow range of 22–27 kJ mol^{-1} . It is particularly note worthy that the Q_{st} for C_2H_2 in PCP-33 is about half the value reported for other MOFs with open metal sites such FeMOF-74, MgMOF-74, CoMOF-74, and CuBTC,⁴² implying the significantly lower energy consumption during regeneration of adsorbed C_2 hydrocarbons in fixed bed adsorbers of PCP-33. This is because the large pore size (9–22 Å) and organic counterions of PCP-33 somewhat reduced the heat of adsorption.⁴³

Transient Breakthroughs. We also performed transient breakthrough simulations in a fixed bed adsorber to investigate the separation potential of PCP-33. Such simulations reflect the combined influences of adsorption selectivity and uptake capacity. The breakthroughs of an equimolar component mixture including CH_4 , C_2H_2 , C_2H_4 , C_2H_6 , and CO_2 , using the methodology described in earlier works,^{44,45} were explored at 298 K. The relative concentrations of outflowing gas are shown in Figure 6. The simulation results for transient breakthrough are presented in terms of a dimensionless time τ , defined by dividing the actual time, t , by the characteristic time ($L\varepsilon/u$). The breakthrough hierarchy is dictated by the adsorption strengths; the weaker the adsorption, the earlier the breakthrough.

Natural gas usually contains CO_2 and C_2 hydrocarbons that require removal by selective adsorption. Figure 6a presents simulation results for equimolar five-component $CH_4/C_2H_2/C_2H_4/C_2H_6/CO_2$ mixtures. The partial pressures of these five gases were set as 20 kPa. It is clear that pure CH_4 can be recovered because it is the least strongly adsorbed component and elutes first. In addition, the result shown in Figure 6b demonstrates that after recovery of CH_4 , the remaining $C_2H_2/C_2H_4/C_2H_6/CO_2$ mixture can be separated to yield two fractions: CO_2 and C_2 hydrocarbons. Thus, we further simulate the separation behavior of C_2H_2/CO_2 , since it is particularly challenging in view of their similarity molecular dimensions and also boiling point.³ In view of the high selectivity for adsorption of C_2H_2 , it is possible to recover pure CO_2 during the adsorption phase in a fixed bed adsorber (Figure 6c). In addition, the significant time interval between the

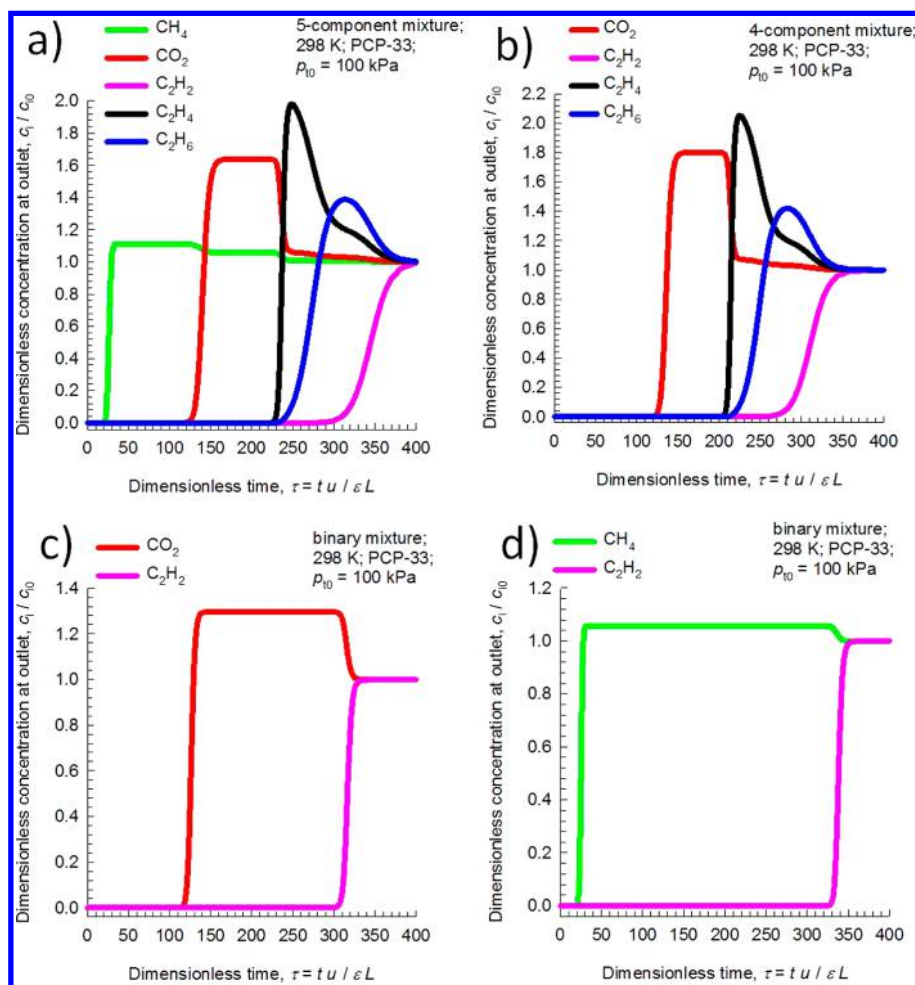


Figure 6. Transient breakthrough simulations for separation of equimolar 5-, 4-, 2-, and 2-component $\text{CH}_4/\text{C}_2\text{H}_2/\text{C}_2\text{H}_4/\text{C}_2\text{H}_6/\text{CO}_2$ mixtures using PCP-33 at 298 K, with partial pressures of 20, 25, 50, and 50 kPa for each component, respectively.

breakthroughs of C_2H_2 and CH_4 in PCP-33 indicates excellent separation at 298 K (Figure 6d).

We now consider $\text{C}_2\text{H}_2/\text{C}_2\text{H}_4$ separations. In steam cracking of C_2H_6 to produce C_2H_4 , one of the byproducts is C_2H_2 . C_2H_2 has a deleterious effect on end-products, such as polyethylene. Therefore, recovery or removal of C_2H_2 from C_2H_4 streams is essential. Typically, C_2H_2 forms about 1% of the C_2H_4 streams, and the impurity level of 40 ppm of C_2H_2 needs to be met for C_2H_4 feed to a polymerization reactor. The selective removal of C_2H_2 is conventionally carried out by absorption in dimethylformamide; this process is energy-intensive. Selective adsorption with PCP-33 could be an energy-efficient alternative. The transient breakthrough simulations for $\text{C}_2\text{H}_2/\text{C}_2\text{H}_4$ (1/99) mixtures are shown in Figure 7. We note that for $\tau < 170$, the outlet gas contains less than 40 ppm of C_2H_2 . The adsorption cycle needs to be terminated at $\tau = 170$ and the regeneration process needs to be initiated. Due to the significantly low binding energy of C_2H_2 in PCP-33, the regeneration costs can be expected to be lower than that of FeMOF-74, MgMOF-74, CoMOF-74, and CuBTC, which are also suitable for this separation task.⁴²

In order to further confirm such high separation capability of PCP-33, pulse chromatographic simulations for varied gas mixtures were carried out. Figure S12, Supporting Information, demonstrates the good potential of PCP-33 for the purification of natural gas. The remaining $\text{C}_2\text{H}_2/\text{C}_2\text{H}_4/\text{C}_2\text{H}_6/\text{CO}_2$ mixture can also be separated to yield two fractions: CO_2 and C2 hydrocarbons. In addition, the separation potential of $\text{CO}_2/\text{C}_2\text{H}_2$ in PCP-33 is clearly indicated. The result of pulse chromatographic simulations match well with that of the breakthrough curves presented in Figure 6.

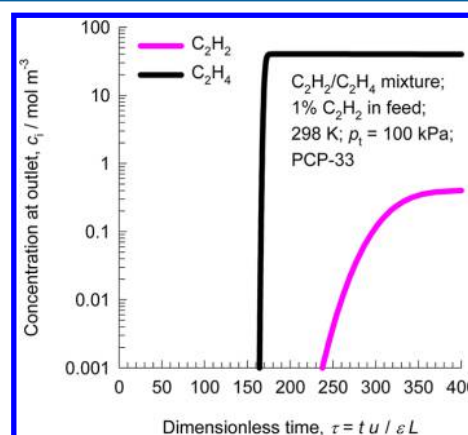


Figure 7. Transient breakthrough of $\text{C}_2\text{H}_2/\text{C}_2\text{H}_4$ mixture containing 1% C_2H_2 mixture in an adsorber bed packed with PCP-33. The partial pressures of C_2H_2 and C_2H_4 in the inlet feed gas mixture are, respectively, $p_1 = 1$ kPa, $p_2 = 99$ kPa.

In Situ Infrared Spectroscopy. Although the average adsorption heat of the isolated frameworks can be estimated by the calculation,^{46,47} exploring the interactions and adsorption behaviors of the guest on each adsorption site becomes more important, since the precise understanding of the information between host and guest will guide the next material design. Indeed, it is better to load C_2H_2 inside the framework for the IR measurements, but because of its

explosion risk, we employed the typical experiment of PCPs loaded with H_2 for the experiments of in situ infrared spectroscopy.⁴⁸

For the pressure-dependent experiments, the in situ IR was collected following the increased pressure from 0 to 5 bar at 102 K. The collected IR spectra revealed clearly of the procedure of the H_2 adsorption in them (Figure S17a, Supporting Information). For PCP-33, the first peak appears at 4128 cm^{-1} and subsequently grows and shifts to 4130 cm^{-1} , with a weak shoulder at $\sim 4100\text{ cm}^{-1}$. The bathochromic frequency shifts, from the gas phase value from Raman spectroscopy (4161 cm^{-1}) of the H–H stretching mode of free H_2 molecule, about to 31 cm^{-1} . Thus, the broad nature of the absorption band is attributed to the presence of the binding environments for H_2 at the Cu^{2+} adsorption sites, owing to the partial solvation of the $[Cu_4Cl]^{7+}$ clusters throughout the material and similarly to what was observed in a recent IR study for open metal center PCPs.^{48–50} Further, temperature-dependent infrared spectra, shown in Figure S17b, Supporting Information, also confirmed this interaction. One bar of H_2 was dosed into the degassed PCP-33 at 102 K, and the IR spectra were collected at intervals of 10 K increased to final temperature of 172 K. During the temperature ramping, the pressure of the sample cell was maintained at 1 bar. The enthalpy of H_2 adsorbed on this site of PCP-33 was calculated by the peak integrals. The high coverage ΔH_{ads} of these sites is around $-4.2\text{ kJ}\cdot\text{mol}^{-1}$, which is lower than that of the adsorption heat of some microframeworks and zeolites.^{50,51} This is because, compared with Mn-BTT, the organic counterions of PCP-33 provide weaker interaction toward guest molecules than Mn^{2+} counterions provide.

Water and Chemical Stability of PCP-33. Encouraged by these interesting characters of PCP-33, we determined its water and chemical stability, because such properties of PCP sorbents are the important factors that will possibly restrict their feasible application.^{35,52–54} Almost 20000 PCP structures have been reported to date; however, very few of them can maintain their porosity after moisture, water, and chemical treatment,^{28,55–57} which is a key challenge for PCP/MOF chemistry. In order to check the stability of PCP-33, fresh crystals were soaked in harsh conditions: hot aqueous HCl (pH = 2), aqueous NaOH (pH = 12), and water solutions for 24 h. After the temperature cooled, we collected the PXRD for each of them. As shown in Figure 8, we found that the PXRD of treated samples are

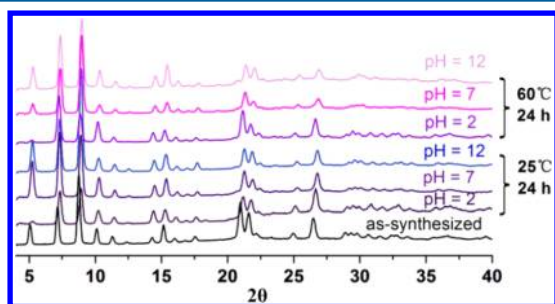


Figure 8. PXRD patterns of water and chemical treated PCP-33.

consistent with their as-synthesized form. Additionally, to further confirm the integrity of the material, CO_2 adsorption isotherms at 195 K for PCP-33 were performed. The gas uptake of treated samples (pH = 2, 7, and 12 at $25\text{ }^\circ\text{C}$; pH = 7 at $60\text{ }^\circ\text{C}$) displaying type I adsorption isotherms are almost same as that of fresh sample. However, the gas uptake of samples that treated under hot aqueous HCl (pH = 2) and aqueous NaOH (pH = 12) decreased very little. Therefore, PCP-33 is a rare sample with good water- and chemical-resistance. Taking the crystal structure and designed ligand into consideration, the high aqueous and chemical stability of PCP-33 should be attributed to the increased coordination bond strength of Cu–N.³⁵

CONCLUSIONS

In conclusion, we utilized a heterodonor ligand containing carboxylate and azolate groups and synthesized a new PCP

(PCP-33). Adsorption experiments, IAST, breakthrough, and pulse chromatographic simulations strongly demonstrate that it has very high potential to purify natural gas, separate C_2H_2/CO_2 mixtures, and selectively capture of C_2H_2 from C_2H_2/C_2H_4 mixtures at room temperature. More importantly, the good water- and chemical-resistance of this framework indicates realizable separation applications. Thus, we can expected that the promising candidate of PCP-33 will not only offer energy efficient separation of small hydrocarbons in the pressure swing adsorption process but also facilitate the next exploration of PCPs with improved functions.

ASSOCIATED CONTENT

Supporting Information

Synthesis and characterization, PXRD, TGA, IR, sorption isotherms, IAST and breakthrough calculations, isotherm fitting parameters, and video animations of transient breakthrough simulations for five-component mixtures for PCP-33. This material is available free of charge via the Internet at <http://pubs.acs.org>.

AUTHOR INFORMATION

Corresponding Author

*E-mail: duanjingui@njtech.edu.cn.

Notes

The authors declare no competing financial interest.

ACKNOWLEDGMENTS

The authors gratefully acknowledge the support from Natural Science Foundation of China (No. 21301148).

REFERENCES

- (1) Stolaroff, J. K.; Bhattacharyya, S.; Smith, C. A.; Bourcier, W. L.; Cameron-Smith, P. J.; Aines, R. D. *Environ. Sci. Technol.* **2012**, *46*, 6455–6469.
- (2) Stang, P. J.; Diederich, F. *Modern Acetylene Chemistry*; VCH: New York, 1995.
- (3) Fischer, M.; Hoffmann, F.; Fröba, M. *ChemPhysChem* **2010**, *11*, 2220–2229.
- (4) Matsuda, R.; Kitaura, R.; Kitagawa, S.; Kubota, Y.; Belosludov, R. V.; Kobayashi, T. C.; Sakamoto, H.; Chiba, T.; Takata, M.; Kawazoe, Y.; Mita, Y. *Nature* **2005**, *436*, 238–241.
- (5) Nugent, P.; Belmabkhout, Y.; Burd, S. D.; Cairns, A. J.; Luebke, R.; Forrest, K.; Pham, T.; Ma, S. Q.; Space, B.; Wojtas, L.; Eddaoudi, M.; Zaworotko, M. J. *Nature* **2013**, *495*, 80–84.
- (6) Li, J. R.; Sculley, J.; Zhou, H. C. *Chem. Rev.* **2012**, *112*, 869–932.
- (7) Bloch, E. D.; Queen, W. L.; Krishna, R.; Zadrozny, J. M.; Brown, C. M.; Long, J. R. *Science* **2012**, *335*, 1606–1610.
- (8) Cinke, M.; Li, J.; Bauschlicher, C. W.; Ricca, A.; Meyyappan, M. *Chem. Phys. Lett.* **2003**, *376*, 761–766.
- (9) Choudhary, V. R.; Mayadevi, S. *Sep. Sci. Technol.* **1993**, *28*, 2197–2209.
- (10) Furukawa, H.; Ko, N.; Go, Y. B.; Aratani, N.; Choi, S. B.; Choi, E.; Yazaydin, A. O.; Snurr, R. Q.; O’Keeffe, M.; Kim, J.; Yaghi, O. M. *Science* **2010**, *329*, 424–428.
- (11) Ma, S. Q.; Sun, D. F.; Simmons, J. M.; Collier, C. D.; Yuan, D. Q.; Zhou, H. C. *J. Am. Chem. Soc.* **2008**, *130*, 1012–1016.
- (12) Kitagawa, S.; Kitaura, R.; Noro, S. *Angew. Chem., Int. Ed.* **2004**, *43*, 2334–2375.
- (13) Lan, Y. Q.; Jiang, H. L.; Li, S. L.; Xu, Q. *Adv. Mater.* **2011**, *23*, 5015–5020.
- (14) Holst, J. R.; Cooper, A. I. *Adv. Mater.* **2010**, *22*, 5212–5216.
- (15) Ferey, G.; Mellot-Draznicks, C.; Serre, C.; Millange, F.; Dutour, J.; Surble, S.; Margiolaki, I. *Science* **2005**, *309*, 2040–2042.

- (16) Bae, Y. S.; Lee, C. Y.; Kim, K. C.; Farha, O. K.; Nickias, P.; Hupp, J. T.; Nguyen, S. T.; Snurr, R. Q. *Angew. Chem., Int. Ed.* **2012**, *51*, 1857–1860.
- (17) Murray, L. J.; Dinca, M.; Long, J. R. *Chem. Soc. Rev.* **2009**, *38*, 1294–1314.
- (18) Lee, J. Y.; Pan, L.; Huang, X. Y.; Emge, T. J.; Li, J. *Adv. Funct. Mater.* **2011**, *21*, 993–998.
- (19) Vaidhyanathan, R.; Iremonger, S. S.; Shimizu, G. K. H.; Boyd, P. G.; Alavi, S.; Woo, T. K. *Science* **2010**, *330*, 650–653.
- (20) Zhang, Y. B.; Zhou, H. L.; Lin, R. B.; Zhang, C.; Lin, J. B.; Zhang, J. P.; Chen, X. M. *Nat. Commun.* **2012**, *3*, No. 642.
- (21) Du, M.; Li, C.; Chen, M.; Ge, Z.; Wang, X.; Wang, L.; Liu, C. J. *Am. Chem. Soc.* **2014**, *136*, 10906–10909.
- (22) Dinca, M.; Han, W. S.; Liu, Y.; Dailly, A.; Brown, C. M.; Long, J. R. *Angew. Chem., Int. Ed.* **2007**, *46*, 1419–1422.
- (23) Ma, S. Q.; Zhou, H. C. *J. Am. Chem. Soc.* **2006**, *128*, 11734–11735.
- (24) Van Humbeck, J. F.; McDonald, T. M.; Jing, X. F.; Wiers, B. M.; Zhu, G. S.; Long, J. R. *J. Am. Chem. Soc.* **2014**, *136*, 2432–2440.
- (25) He, Y. B.; Zhang, Z. J.; Xiang, S. C.; Fronczek, F. R.; Krishna, R.; Chen, B. L. *Chem.—Eur. J.* **2012**, *18*, 613–619.
- (26) Geier, S. J.; Mason, J. A.; Bloch, E. D.; Queen, W. L.; Hudson, M. R.; Brown, C. M.; Long, J. R. *Chem. Sci.* **2013**, *4*, 2054–2061.
- (27) Duan, J. G.; Higuchi, M.; Krishna, R.; Kiyonaga, T.; Tsutsumi, Y.; Sato, Y.; Kubota, Y.; Takata, M.; Kitagawa, S. *Chem. Sci.* **2014**, *5*, 660–666.
- (28) Duan, J. G.; Higuchi, M.; Horike, S.; Foo, M. L.; Rao, K. P.; Inubushi, Y.; Fukushima, T.; Kitagawa, S. *Adv. Funct. Mater.* **2013**, *23*, 3525–3530.
- (29) Duan, J. G.; Yang, Z.; Bai, J. F.; Zheng, B. S.; Li, Y. Z.; Li, S. H. *Chem. Commun.* **2012**, *48*, 3058–3060.
- (30) Du, M.; Chen, M.; Yang, X.; Wen, J.; Wang, X.; Fang, S.; Liu, C. *J. Mater. Chem. A* **2014**, *2*, 9828–9834.
- (31) Britt, D.; Furukawa, H.; Wang, B.; Glover, T. G.; Yaghi, O. M. *Proc. Natl. Acad. Sci. U.S.A.* **2009**, *106*, 20637–20640.
- (32) McDonald, T. M.; D'Alessandro, D. M.; Krishna, R.; Long, J. R. *Chem. Sci.* **2011**, *2*, 2022–2028.
- (33) Demessence, A.; D'Alessandro, D. M.; Foo, M. L.; Long, J. R. *J. Am. Chem. Soc.* **2009**, *131*, 8784–8785.
- (34) Yuan, D. Q.; Zhao, D.; Sun, D. F.; Zhou, H. C. *Angew. Chem., Int. Ed.* **2010**, *49*, 5357–5361.
- (35) Choi, H. J.; Dinca, M.; Dailly, A.; Long, J. R. *Energy Environ. Sci.* **2010**, *3*, 117–123.
- (36) Makal, T. A.; Wang, X.; Zhou, H. C. *Cryst. Growth Des.* **2013**, *13*, 4760–4768.
- (37) Ma, D. Y.; Li, Y. W.; Li, Z. *Chem. Commun.* **2011**, *47*, 7377–7379.
- (38) Duan, J. G.; Higuchi, M.; Foo, M. L.; Horike, S.; Rao, K. P.; Kitagawa, S. *Inorg. Chem.* **2013**, *52*, 8244–8249.
- (39) Dinca, M.; Dailly, A.; Liu, Y.; Brown, C. M.; Neumann, D. A.; Long, J. R. *J. Am. Chem. Soc.* **2006**, *128*, 16876–16883.
- (40) Spek, A. L. *J. Appl. Crystallogr.* **2003**, *36*, 7–13.
- (41) Myers, A. L.; Prausnitz, J. M. *AIChE J.* **1965**, *11*, 121–130.
- (42) He, Y.; Krishna, R.; Chen, B. *Energy Environ. Sci.* **2012**, *5*, 9107–9120.
- (43) Klein, N.; Senkovska, I.; Gedrich, K.; Stoeck, U.; Henschel, A.; Mueller, U.; Kaskel, S. *Angew. Chem., Int. Ed.* **2009**, *48*, 9954–9957.
- (44) Krishna, R. *Microporous Mesoporous Mater.* **2014**, *185*, 30–50.
- (45) Krishna, R.; Long, J. R. *J. Phys. Chem. C* **2011**, *115*, 12941–12950.
- (46) Rowsell, J. L. C.; Yaghi, O. M. *J. Am. Chem. Soc.* **2006**, *128*, 1304–1315.
- (47) Sumida, K.; Stuck, D.; Mino, L.; Chai, J. D.; Bloch, E. D.; Zavorotynska, O.; Murray, L. J.; Dinca, M.; Chavan, S.; Bordiga, S.; Head-Gordon, M.; Long, J. R. *J. Am. Chem. Soc.* **2013**, *135*, 1083–1091.
- (48) Vitillo, J. G.; Regli, L.; Chavan, S.; Ricchiardi, G.; Spoto, G.; Dietzel, P. D. C.; Bordiga, S.; Zecchina, A. *J. Am. Chem. Soc.* **2008**, *130*, 8386–8396.
- (49) Peterson, V. K.; Liu, Y.; Brown, C. M.; Kepert, C. J. *J. Am. Chem. Soc.* **2006**, *128*, 15578–15579.
- (50) Areal, C. O.; Chavan, S.; Cabello, C. P.; Garrone, E.; Palomino, G. T. *ChemPhysChem* **2010**, *11*, 3237–3242.
- (51) Palomino, G. T.; Bonelli, B.; Areal, C. O.; Parra, J. B.; Carayol, M. R. L.; Armandi, M.; Ania, C. O.; Garrone, E. *Int. J. Hydrogen Energy* **2009**, *34*, 4371–4378.
- (52) Colombo, V.; Galli, S.; Choi, H. J.; Han, G. D.; Maspero, A.; Palmisano, G.; Masciocchi, N.; Long, J. R. *Chem. Sci.* **2011**, *2*, 1311–1319.
- (53) Park, K. S.; Ni, Z.; Cote, A. P.; Choi, J. Y.; Huang, R. D.; Uribe-Romo, F. J.; Chae, H. K.; O'Keeffe, M.; Yaghi, O. M. *Proc. Natl. Acad. Sci. U.S.A.* **2006**, *103*, 10186–10191.
- (54) Taylor, J. M.; Dawson, K. W.; Shimizu, G. K. H. *J. Am. Chem. Soc.* **2013**, *135*, 1193–1196.
- (55) Cychoz, K. A.; Matzger, A. J. *Langmuir* **2010**, *26*, 17198–17202.
- (56) Kandiah, M.; Nilsen, M. H.; Usseglio, S.; Jakobsen, S.; Olsbye, U.; Tisel, M.; Larabi, C.; Quadrelli, E. A.; Bonino, F.; Lillerud, K. P. *Chem. Mater.* **2010**, *22*, 6632–6640.
- (57) Feng, D. W.; Gu, Z. Y.; Li, J. R.; Jiang, H. L.; Wei, Z. W.; Zhou, H. C. *Angew. Chem., Int. Ed.* **2012**, *51*, 10307–10310.